ENVIRONMENTAL EPIGENETICS

Environmental Epigenetics, 2025, **11(1)**, 1–9
DOI: https://doi.org/10.1093/eep/dvaf002
Advance Access Publication 17 March 2025
**RESEARCH ARTICLE**

# Exosomal miR-34b-3p upregulated in response to hypoxia preconditioning modulates circadian rhythms through the targeting of Clock

**Yiquan Yan[1,2,3], Fengzhou Liu[4,‡], Tongmei Zhang[4,‡], Lu Zhao[2], Yateng Tie[3], Rui Wang[3], Qi Yang[5], Jin Ma[1,*], Xingcheng Zhao[3,*]**

[1]Department of Aerospace Physiology, School of Aerospace Medicine, Fourth Military Medical University, Xi'an 710032, China
[2]Department of internal medicine, Hospital of Unit 96608, PLA, Hanzhong 723000, China
[3]Department of Aerospace Medical Training, School of Aerospace Medicine, Fourth Military Medical University, Xi'an 710032, China
[4]Aerospace Clinical Medical Center, School of Aerospace Medicine, Fourth Military Medical University, Xi'an 710032, China
[5]Graduate School, Xinjiang Medical University, Urumqi 830054, China

[‡]These authors contributed equally to this work.
*Corresponding author. Xingcheng Zhao, Department of Aerospace Medical Training, School of Aerospace Medicine, Fourth Military Medical University, Changle West Road 169#, Xi'an 710032, P.R.China. E-mail: zhaoxc@fmmu.edu.cn; Jin Ma, Department of Aerospace Physiology, School of Aerospace Medicine, Fourth Military Medical University, Changle West Road 169#, Xi'an 710032, P.R.China. E-mail: jin-ma@fmmu.edu.cn

## Abstract

The relationship between circadian rhythm disorders and the development of various diseases appears to be significant, with limited current interventions available. Research literature suggests that hypoxia may influence the expression of clock genes and the shifting of rhythm phases. However, the precise mechanisms underlying the modulation of circadian rhythm through circulating exosomes by hypoxia preconditioning remain unclear. In this study, the mice were exposed to hypobaric conditions, simulating an altitude of 5000 m, for 1 h daily over the course of 1 week in order to achieve hypoxia preconditioning. Compared to the control group, no significant alteration was observed in the concentration, modal size, and mean size of circulating exosomes in hypoxia preconditioning mice. Exosomes derived from hypoxia preconditioning effectively suppressed the expression of *Per1*, *Clock*, and *Bmal1* in NIH 3T3 cells. The miRNA sequencing analysis revealed miR-34b-3p as a potential regulator of the *Clock*, resulting in the downregulation of clock gene expression and subsequent promotion of proliferation and migration in NIH 3T3 cells. This study elucidated a novel mechanism of hypoxia preconditioning in the regulation of circadian rhythm, proposing that exosomal miR-34b-3p functions as an unrecognized molecule entity involved in the modulation of circadian rhythm. These findings offer a new avenue for developing protective strategies and therapeutic targets for circadian rhythm disorders.

**Keywords:** hypoxia; circadian rhythms; exosome; Clock; miR-34b-3p

## Introduction

The circadian rhythm is an endogenous and entrainable biological process that oscillates on ∼24-h cycle [1, 2]. This rhythm is synchronized with external time through the influence of light, diet, and various other factors. The disruption of this synchronization can give rise to significant physiological consequences and potentially result in disease [3, 4]. The central regulatory mechanism of the mammalian biological clock involves a transcriptional translation feedback loop governed by the transcriptional activator CLOCK-BMAL1 and the transcriptional suppressor PER-CRY. *CLOCK* (circadian locomotor output cycles kaput), *BMAL1* (brain and muscle arnt-like 1), *PER* (period, including *PER1*, *PER2*, and *PER3*), and *CRY* (cryptochrome, including *CRY1* and *CRY2*) are considered the fundamental clock genes in mammals. The CLOCK and BMAL1 proteins combine to create heterodimers that bind to the promoter E-box of *PER* and *CRY* genes, ultimately facilitating the expression of *PER* and *CRY*. Following translation, the resulting PER and CRY proteins form a heterodimer that inhibits the activation of the CLOCK–BMAL1 dimer and subsequently reducing their own expression, thereby establishing a negative feedback loop [5, 6].

Research findings have indicated that the hypoxia pathway's key component, hypoxia-inducible factor (HIF), exhibits structural similarities with the core clock activators CLOCK and BMAL1, both of which contains PER-ARNT-SIM (PAS) domains. This structural resemblance implies the potential for functional overlap or coordinated regulation between these two pathways [7, 8]. In recent years, researchers have discovered the phenomenon of circadian

Received 7 August 2024; Revised 7 January 2025; Accepted 17 February 2025

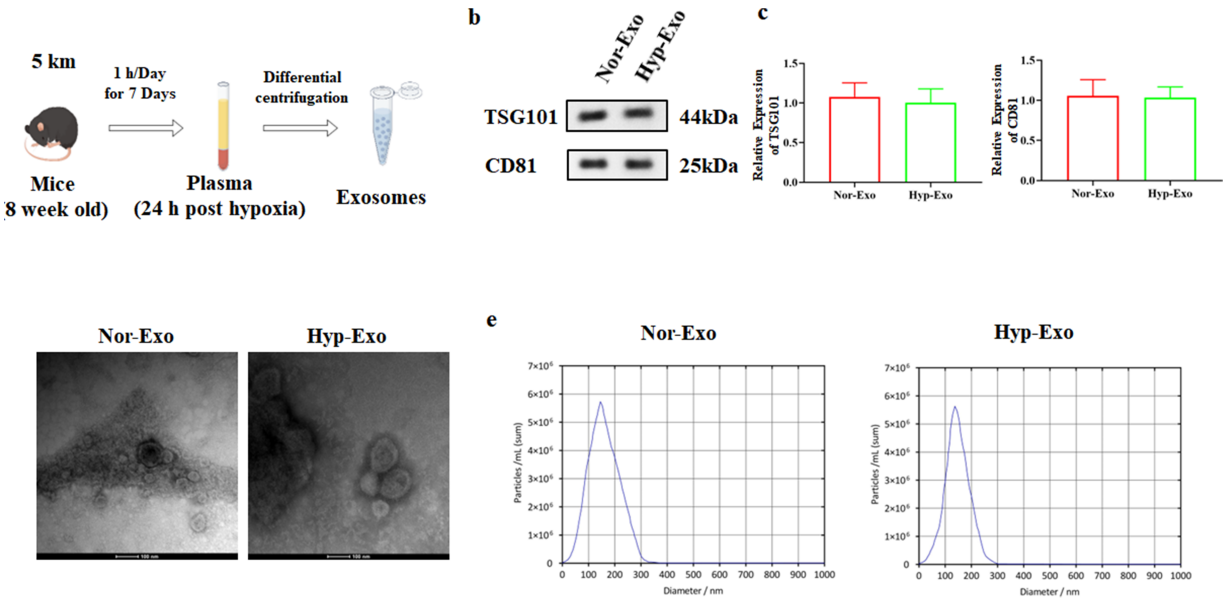


**Figure 1.** There was no significant alteration observed in the quantity of exosomes present in mouse plasma following hypoxia preconditioning. (a). Mouse exosomes extraction diagram. (b). The expressions of exosome markers TSG101 and CD81 were detected by Western blotting from normal (Nor-Exo) or hypoxia preconditioning (Hyp-Exo) mouse plasma. (c). Quantified data obtained from Western blotting. (d). Representative images of exosome morphology from Nor-Exo or Hyp-Exo observed by transmission electron microscopy. (e). Representative results of nanoparticle tracking analysis demonstrating size distribution of exosomes purified from Nor-Exo or Hyp-Exo. $n = 4$. Data present mean ± SEM. One-way ANOVA analysis followed by Dunnett multiple comparisons test.

gating, wherein core clock genes regulate the expression levels of HIF-1a and its downstream target genes, including *GLUT1*, *VEGFA*, *EPO*, and *EGLN1-3*. This regulation is particularly pronounced at the ZT6-9 phase, indicating the involvement of the circadian clock in controlling the hypoxia pathway [9]. Furthermore, the team demonstrated that hypoxic signals can influence the circadian clock's periodicity and amplitude [10, 11].

Numerous studies have demonstrated that hypoxia preconditioning (HPC) can elicit the body's compensatory response to enhance cellular and tissue tolerance to hypoxic conditions, and promoting resilience against prolonged or severe hypoxia. This protective mechanism has been observed in vital organs such as the heart, brain, lung, and kidney [12–14]. Recent experiments have identified a correlation between fluctuations in oxygen levels and the expression of cell clock genes. Administration of a low concentration of oxygen in a murine model of jet lag has been shown to facilitate the adjustment of circadian rhythm phase post-jet lag and expedite adaptation to a new time rhythm. This implies a potential protective role of low oxygen levels in mitigating the effects of jet lag or night shift work [10, 11, 15]. However, the precise impact of low oxygen concentration on resetting the biological clock rhythm and its specific influence on circadian rhythmic behavior remain unclear, necessitating further investigation for validation.

Exosomes, characterized by a double plasma membrane structure, are actively released from cells via exocytosis. They are secreted by various cell types, including dendritic cells, tumor cells, and fibroblasts, and are present in a variety of bodily fluids such as peripheral blood, urine, and saliva [16–18]. Studies have revealed that exosomes are enriched with lipids such as cholesterol, sphingomyelin, and ceramides on their surface, while harboring a diverse array of biologically molecules such as proteins, mRNA, and miRNA derived from the parent cell [19, 20]. Research has demonstrated that hypoxia has the ability to modulate exosome secretion and induce notable alterations in the composition and functionality of exosomes [21–23]. The potential of hypoxia preconditioning to modulate clock gene expression through the regulation of miRNA changes within exosomes, thereby influencing circadian rhythm phase shifts, remains uncertain. This study aims to investigate this issue.

## Results

### There was no significant alteration observed in the quantity of exosomes present in mouse plasma following hypoxia preconditioning

Initially, the study examined the impact of hypoxia preconditioning on the levels and size distribution of circulating exosomes. Peripheral blood exosomes were isolated 24 h post the final hypoxia pretreatment in mice (**Fig. 1a**). Western blot analysis of exosome marker proteins TSG101 and CD81 confirmed successful exosome extraction via ultracentrifugation, no significant disparity in exosome content between the hypoxia pretreatment group and the control group (**Fig. 1b and c**). The morphology of exosomes was examined using transmission electron microscopy, which revealed a similarity in morphology between the experimental and control groups (**Fig. 1d**). Nanoparticle tracking analysis (NTA) further demonstrated that the diameter distribution of extracted extracellular vesicles fell within the range of 300 nm, with no significant disparities in concentration, modal size, and mean size of circulating exosomes between the hypoxia pretreatment training group and the control group mice (**Fig. 1e**).

### The impact of hypoxia preconditioning on the regulation of clock gene expression in NIH 3T3 cells

In order to investigate the impact of hypoxia pretreatment on the expression of cell clock genes, NIH 3T3 cells were exposed to a 4-h period of hypoxia, followed by real-time quantitative PCR analysis

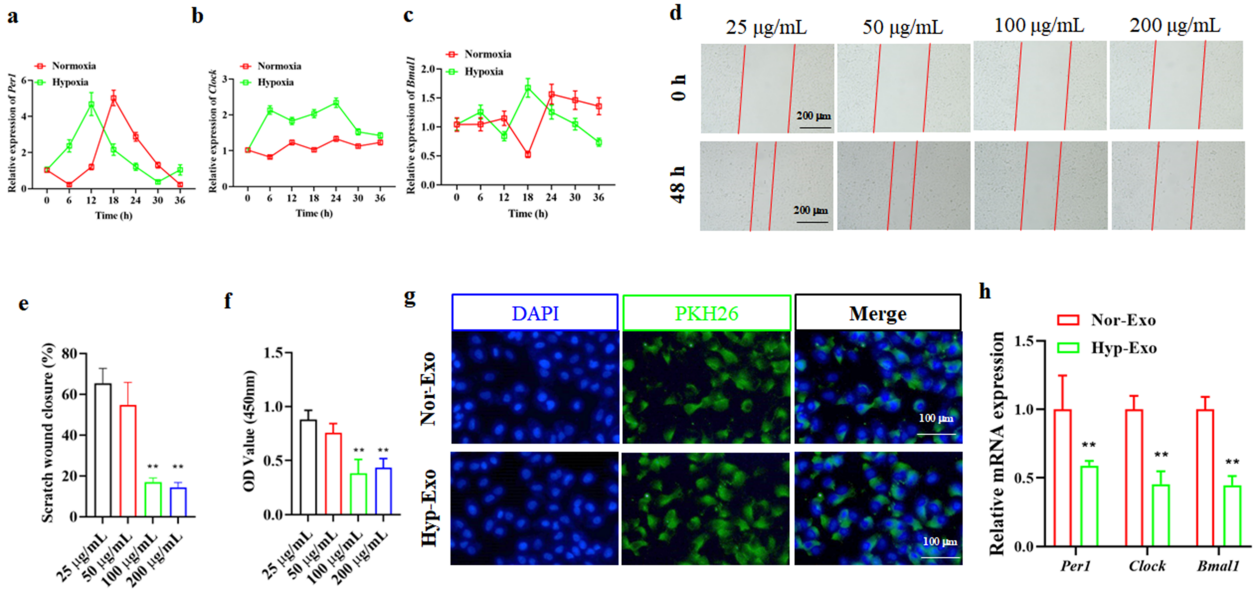


**Figure 2.** Exosomes isolated from mice subjected to hypoxia preconditioning exhibit inhibitory effects on the expression of clock genes in NIH 3T3 cells. (a) The expression of *Per1* was detected by real-time quantitative PCR from NIH 3T3 cells of normal or hypoxia preconditioning. (b) The expression of *Clock* was detected by real-time quantitative PCR from NIH 3T3 cells of normal or hypoxia preconditioning. (c) The expression of *Bmal1* was detected by real-time quantitative PCR from NIH 3T3 cells of normal or hypoxia preconditioning. (d) The effects of 25, 50, 100, 200 μg/ml exosomes on NIH 3T3 cell migration were detected by wound healing assay. (e) Statistical results of wound healing assay from (d). (f) The effects of 25, 50, 100, 200 μg/ml exosomes on NIH 3T3 cell proliferation were detected by CCK-8 assay. (g) The uptake of exosomes derived from normal (Nor-Exo) or hypoxia-preconditioned (Hyp-Exo) mice by NIH 3T3 cells was assessed through immunofluorescence staining, with DAPI used to label the cell nuclei and PKH26 used to label the exosomes. (h) The expression of *Per1*, *Clock*, and *Bmal1* was detected by real-time quantitative PCR from NIH 3T3 cells co-cultured with exosomes of normal (Nor-Exo) or hypoxia-preconditioned (Hyp-Exo) mice. $^{**}P < .01$. $n = 4$. Data present mean ± SEM. Two-way ANOVA analysis followed by Tukey multiple comparisons test used in (e) and (f). One-way ANOVA analysis followed by Dunnett multiple comparisons test used in (h).

for the detection of *Per1*, *Clock*, and *Bmal1* clock gene expression. The results indicated that hypoxia pretreatment does not alter the peak expression levels of *Per1* and *Bmal1*, but it does exert an influence on the rhythmic phase of their expression (**Fig. 2a and c**). In the case of *Clock*, hypoxic pretreatment has exerted a concurrent influence on the circadian phase of its peak expression, with a significant upregulation observed in *Clock* expression (**Fig. 2b**).

## Exosomes isolated from mice subjected to hypoxia preconditioning exhibit inhibitory effects on the expression of clock genes in NIH 3T3 cells

In the most previous literature, 50 μg/ml or 100 μg/ml was selected as the concentration of exosomes to treat cells [24, 25]. To explore the concentration of exosome-treated cells, some scholars have utilized cell proliferation and migration experiments [26, 27]. In order to assess the concentration of circulating exosomes on NIH 3T3 cells, we employed the CCK-8 assay to evaluate cell proliferation and the scratch assay to assess cell migration. The findings from the CCK-8 assay indicated that a concentration of 100 μg/ml of exosomes effectively suppressed the proliferation of NIH 3T3 cells (**Fig. 2f**). Similarly, results from the scratch assay demonstrated that a concentration of 100 μg/ml of extracellular vesicles significantly impeded the migration of NIH 3T3 cells (**Fig. 2d and e**). Consequently, for subsequent investigations, the concentration of exosomes was determined to be 100 μg/ml.

Subsequently, our study aims to investigate the impact of hypoxia preconditioning on clock gene expression in NIH 3T3 cells through exosomes derived from mice. These exosomes are known to contain a substantial quantity of bioactive molecules, which are released by cells upon exosome ingestion, thereby modulating cellular activities. Thus, an initial step in our research involves assessing the uptake of exosomes by NIH 3T3 cells. To achieve this, exosomes isolated from plasma were labeled with green fluorescent dye PKH26 and introduced into NIH 3T3 cell culture dishes, followed by a 6-h incubation period in a cell incubator. The findings from immunofluorescence staining revealed a substantial presence of green fluorescence within the cells (**Fig. 2g**), suggesting that the internalization of exosomes followed a 6-h co-culture with NIH 3T3 cells. Additionally, results obtained from real-time quantitative PCR demonstrated that exosomes derived from hypoxia preconditioning effectively suppressed the expression of *Per1*, *Clock*, and *Bmal1* in NIH 3T3 cells (**Fig. 2h**).

## The gene *Clock* is a target of miR-34b-3p

To investigate the regulatory mechanism underlying hypoxia preconditioning in mouse exosomes on the clock gene expression in NIH 3T3 cells, we performed miRNA sequencing analysis on the exosomes. The gene expression heatmap showed the most significant changes in the 20 miRNA molecules, including 10 upregulated and 10 downregulated (**Fig. 3a**). The volcano plot shows the overall situation of differentially expressed miRNAs (**Fig. 3b**). The expression levels of the top 10 significantly upregulated miRNAs were validated. Subsequent real-time quantitative PCR analysis confirmed a significant upregulation of all 10 miRNAs in the exosomes derived from hypoxic preconditioned mice, consistent with the sequencing findings (**Fig. 4a**). We selected miR-34b-3p with significant changes from them. We detected the expression of miR-34b-3p in hypothalamus, pineal gland, hippocampus, and cerebral

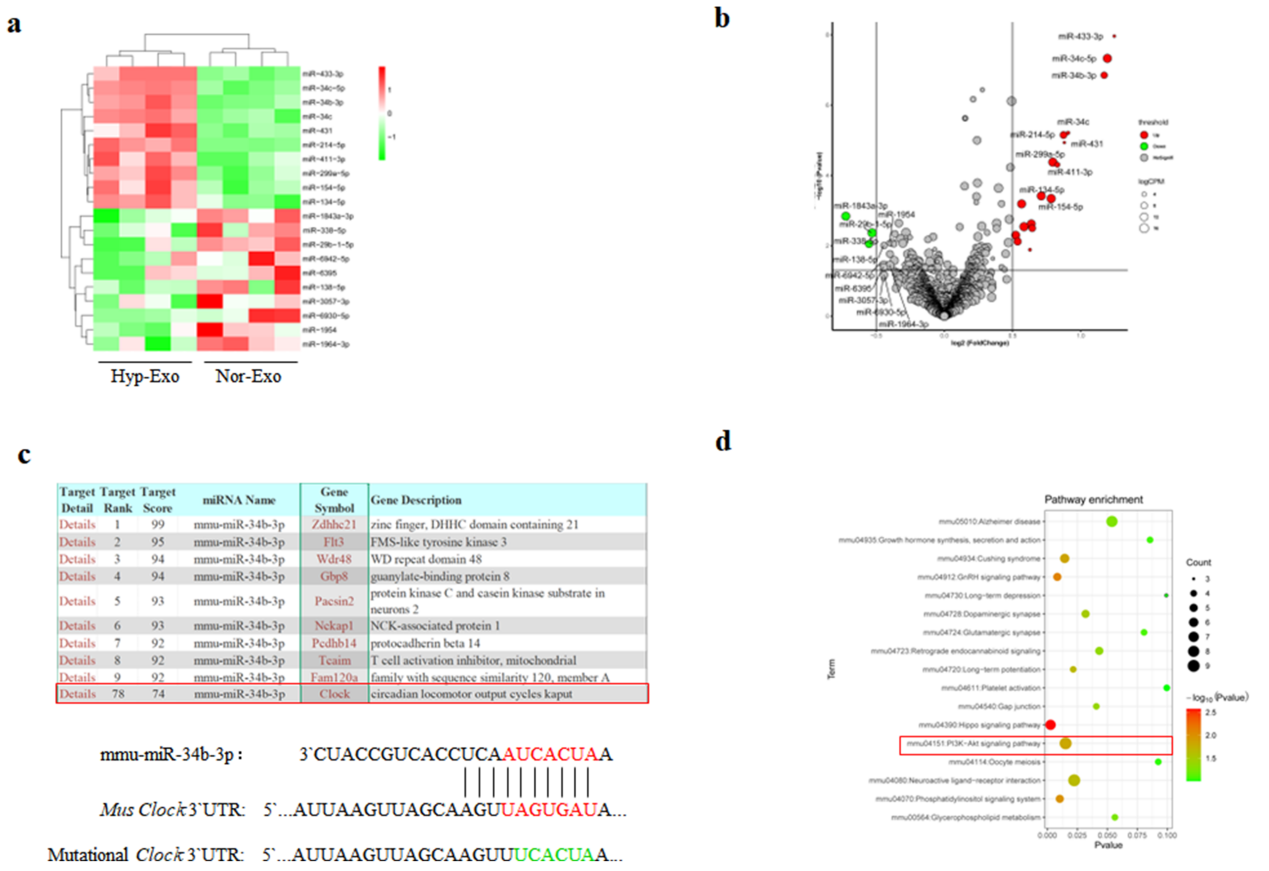


**Figure 3.** miRNA sequencing and bioinformatics analysis. (a) Heat map of miRNAs sequencing results from exosomes of normal (Nor-Exo) or hypoxia-preconditioned (Hyp-Exo) mice. (b) Volcano map of miRNAs sequencing results from exosomes of normal (Nor-Exo) or hypoxia-preconditioned (Hyp-Exo) mice. (c) Prediction analysis of miR-34b-3p target genes, with the *Clock* gene circled . The bottom is alignment of miR-34b-3p sequence with target site of the 3′ UTR of *Clock* mRNA. Complementary sequences were indicated with vertical line. Seed sequences were indicated with red lettering and mutational sequences were indicated with green lettering. (d) Enrichment analysis of miR-34b-3p target genes, with the PI3K/Akt signaling pathway circled. $n = 4$.

cortex from hypoxia treated and normal mice by real-time quantitative PCR analysis. The results showed that the expression of miR-34b-3p was significantly up-regulated in hypothalamus and pineal gland, while no significant change was observed in hippocampus and cerebral cortex (**Fig. 4b**). Therefore, we believed that up-regulated miR-34b-3p was mainly from hypothalamus and pineal gland. To ascertain the principal miRNA, computational tools were employed to forecast the potential binding of miR-34b-3p to the 3'UTR of *Clock* (**Fig. 3c**). KEGG pathway analysis showed that the miR-34b-3p target genes are more enriched in the PI3K-AKT signaling pathway (**Fig. 3d**). Therefore, in terms of subsequent molecular mechanisms, we focused on detecting the expression changes of PI3K/AKT signaling pathway related molecules.

Subsequent Western blot analysis revealed a noteworthy reduction in CLOCK expression in exosomes obtained from hypoxic preconditioned mice compared to the control group, suggesting a potential correlation with the elevated levels of miR-34b-3p within these exosomes (**Fig. 4c and d**). The findings from the dual luciferase reporter gene assay demonstrated that miR-34b-3p exerts a significant inhibitory effect on the fluorescence intensity of the dual luciferase reporter gene system incorporating wild-type (wt) *Clock* sequences, but not on the system containing *Clock* mutated sequences (mut) (**Figs. 3c** and **4e**). This suggests that *Clock* serves as a target gene for miR-34b-3p.

## The molecule miR-34b-3p plays a pivotal role in the regulation of clock gene expression, proliferation, and migration within exosomes in NIH 3T3 cells

The PI3K/Akt signaling pathway plays a crucial role in cell survival and proliferation. In order to elucidate the impact of miR-34b-3p on NIH 3T3 cells, we examined the regulatory influence of miR-34b-3p on PI3K/Akt signaling. Our Western blotting analysis revealed that the overexpression of miR-34b-3p significantly enhanced the phosphorylation levels of p-PI3K and p-Akt, while leaving the expression levels of PI3K and Akt unaltered compared to the mimic NC group. The inhibition of miR-34b-3p significantly attenuates the phosphorylation levels of p-PI3K and p-Akt, while exerting no impact on the expression of PI3K and Akt proteins (**Fig. 5a-c**). These findings indicate that miR-34b-3p plays a role in enhancing the survival signal of the PI3K/Akt pathway in NIH 3T3 cells. Subsequently, cells were transfected with inhibitors targeting miR-34b-3p by lipofectamine before adding exosomes obtained from hypoxia preconditioning mice. The findings demonstrated that exosomes obtained from hypoxic preconditioned mice effectively increased the proliferation and migration of NIH 3T3 cells, while this inhibitory effect was attenuated by the miR-34b-3p inhibitor (**Fig. 5d-f**). The findings from real-time quantitative PCR analysis indicated that the inhibition of miR-34b-3p could counteract the suppression of *Per1*, *Clock*, and *Bmal1* gene

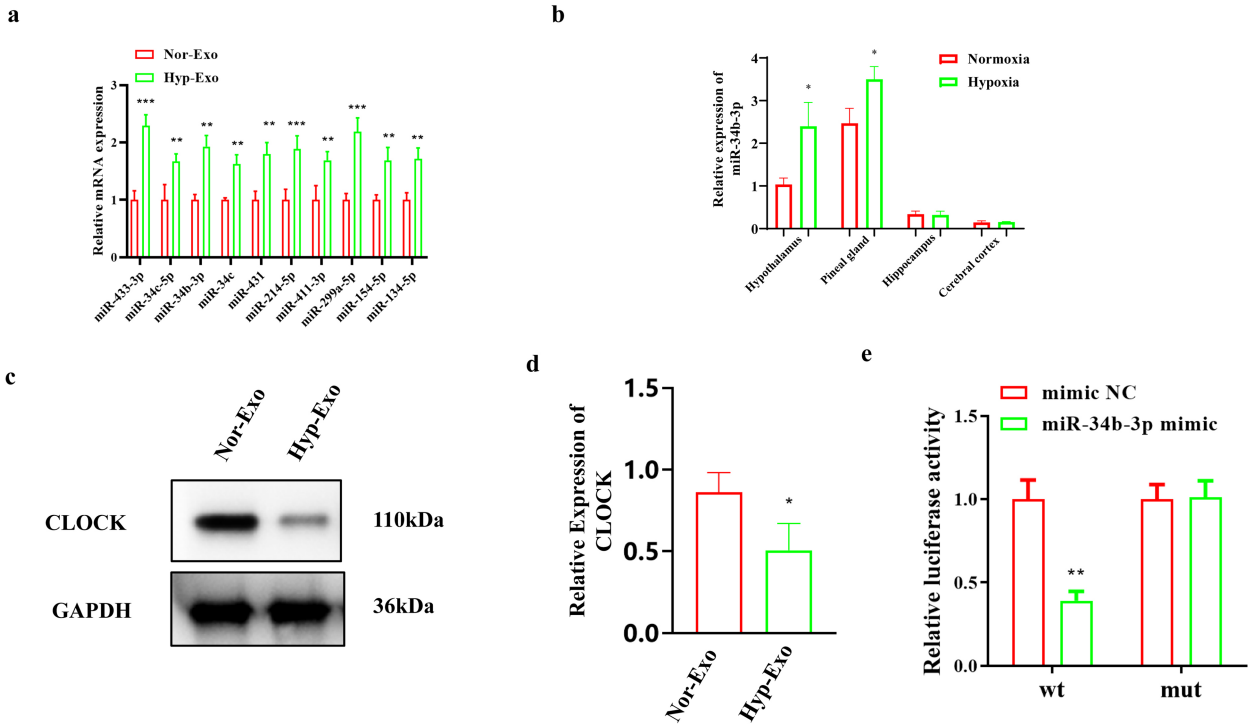


**Figure 4.** The gene *Clock* is a target of miR-34b-3p. (a) Real-time quantitative PCR was employed to identify 10 microRNAs that exhibited significant upregulation in the sequencing data. (b) The expression of miR-34b-3p in hypothalamus, pineal gland, hippocampus, and cerebral cortex from hypoxia treated and normal mice by real-time quantitative PCR analysis. (c) Following treatment of NIH 3T3 cells with exosomes derived from normal and hypoxic preconditioned mice, the expression of the CLOCK protein was assessed using Western blotting analysis. (d) Statistical results from Western blotting in (c). (e) The direct regulatory relationship between miR-34b-3p and *Clock* was detected using a dual luciferase reporter gene assay. $^{*}P < .05$, $^{***}P < .001$. $n = 4$. Data present mean ± SEM. One-way ANOVA analysis followed by Dunnett multiple comparisons test.

expression in NIH 3T3 cells induced by exosomes derived from hypoxia preconditioning mice (**Fig. 5g**). These results suggest that miR-34b-3p plays a crucial role in regulating clock gene expression, proliferation, and migration in NIH 3T3 cells via exosomal communication.

## Discussion

This research utilized a hypoxia preconditioning mouse model to investigate the effects of circulating exosomes on clock gene expression, cell proliferation, and migration. The study yielded two novel discoveries: firstly, the circulating exosomes induced by hypoxia preconditioning, which contain bioactive substances, were found to modulate the expression of clock genes and circadian rhythms. Furthermore, miR-34b-3p has been identified as a crucial factor in the modulation of clock gene expression within circulatory exosomes following hypoxia preconditioning, thereby exerting influence on circadian rhythm through targeted regulation of *Clock* expression. This investigation elucidates a novel pathway by which hypoxia preconditioning modulates circadian rhythms through the regulation of circulating exosomes, emphasizing the significance of miR-34b-3p as a novel regulator of circadian processes.

Our research group previously conducted a study on the impact of hypoxia preconditioning on human susceptibility to motion sickness. The results showed that after one week of hypoxia preconditioning, participants showed a significant reduction in motion sickness symptoms induced by electric rotary chair, indicating that hypoxia preconditioning has a certain protective effect on the stability of vestibular function in the human body. In order to minimize the occurrence of high-altitude decompression sickness and ensure the safety of the subjects, we chose an altitude of 3 km as the hypoxia condition for the human body [28]. In this study, we performed hypoxia preconditioning in mice. In order to achieve better hypoxia preconditioning effects, we chose a 5 km hypoxic condition, which is also 1 hour of continuous hypoxia preconditioning per day for 1week.

Utilizing NTA technology for exosome size detection, our study revealed that although there was no statistically significant variance in the modal and mean sizes of circulating exosomes between hypoxia pretreatment and control group mice, the distribution curve indicated a more homogeneous diameter of circulating exosomes in the hypoxia pretreatment group. This resulted in a reduction of both larger and smaller extracellular vesicles, potentially influencing clock gene expression. Research reports have indicated that utilizing NTA technology to detect aerobic exercise in rats did not result in significant changes in model and mean sizes. However, the experimental group exhibited similar alterations in circulating exosomes as observed in our own research findings [29].

MicroRNAs (miRNAs) are known to exert a regulatory role in post-transcriptional translation by either inhibiting or degrading the mRNAs of target genes [30]. In this study, we identified key miRNAs involved in the regulation of NIH 3T3 cell circadian rhythm genes through the analysis of exosomes derived from hypoxic pre-adapted mice. The top 10 up-regulated miRNAs exhibiting the most significant alterations were selected, and their predicted miRNA targets were further validated using the miRDB and TargetScan database. The identification of miR-34b-3p as a potential regulator of the 3′ untranslated region (UTR) of the *Clock*

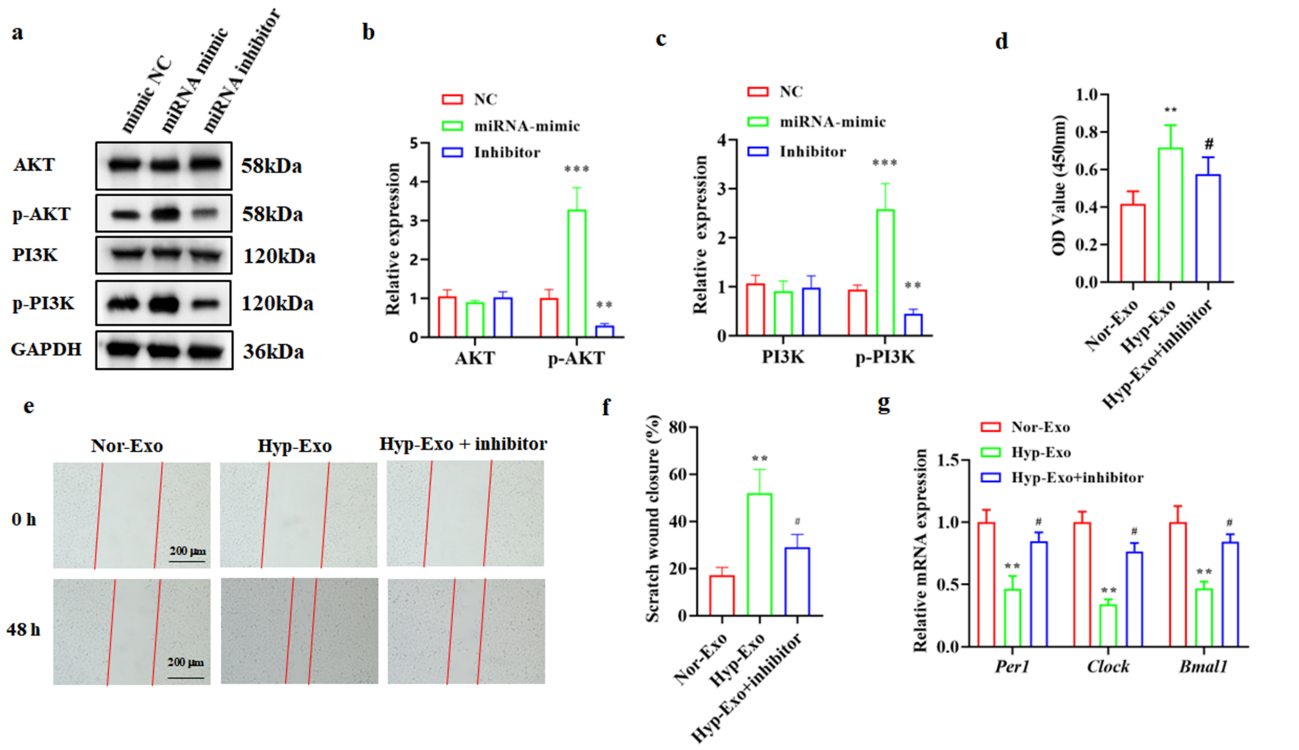


**Figure 5.** The molecule miR-34b-3p plays a pivotal role in the regulation of NIH 3T3 clock gene expression, proliferation, and migration within exosomes. (a) The levels of AKT, p-AKT, PI3K, and p-PI3K proteins in NIH 3T3 cells treated with NC, miR-34b-3p mimic, or miR-34b-3p inhibitor were evaluated through Western blotting analysis, with GAPDH serving as the internal control. (b) Statistics of AKT and p-AKT expression in (a). (c) Statistics of PI3K and p-PI3K expression in (a). (d) The effects of Nor-Exo, Hyp-Exo, or Hyp-Exo + miR-34b-3p inhibitor on NIH 3T3 cell proliferation were detected by CCK-8 assay. (e) The effects of Nor-Exo, Hyp-Exo, or Hyp-Exo + miR-34b-3p inhibitor on NIH 3T3 cell migration were detected by wound healing assay. (f) Statistical results of wound healing assay from (e). (g) The expression of *Per1*, *Clock*, and *Bmal1* was detected by real-time quantitative PCR from NIH 3T3 cells treated with Nor-Exo, Hyp-Exo, or Hyp-Exo + miR-34b-3p inhibitor. $^{**}P < .01$ compared with NC or Nor-Exo, $^{***}P < .001$ compared with NC or Nor-Exo, $^{\#}P < .05$ compared with Hyp-Exo. $n = 4$. Data present mean ± SEM. Two-way ANOVA analysis followed by Tukey multiple comparisons test.

gene was supported by subsequent experiments using double luciferase reporter assays, which demonstrated that miR-34b-3p effectively suppressed *Clock* expression by directly targeting it. We also screened for other differentially expressed miRNAs such as miR-433-3p and miR-34c-5p (**Fig. 3a and b**), but target gene predictions showed that their target genes did not include clock genes.

Several limitations were identified in our study. Firstly, we observed an increase in the content of miR-34b-3p in mouse circulating exosomes following hypoxia preconditioning. However, owing to the intricate nature of exosome miRNA packaging and the current inability to selectively isolate exosomes from specific cell types, the tissue origin of miR-34b-3p in circulating exosomes remains uncertain. Secondly, our study primarily relied on cell experiments for functional verification, lacking evidence from animal experiments. In the subsequent phase, further comprehensive research involving animal models is required.

**Table 1.** Primers used for quantitative real-time PCR analysis

| Target | Forward primer | Reverse primer |
|---|---|---|
| Clock | ATGGTGTTTACCGTAAGCTGTAG | CTCGCGTTACCAGGAAGCAT |
| Bmal1 | TGACCCTCATGGAAGGTTAGAA | GGACATTGCATTGCATGTTGG |
| Per1 | CGGATTGTCTATATTTCGGAGCA | TGGGCAGTCGAGATGGTGTA |
| GAPDH | AATGGATTTGGACGCATTGGT | TTTGCACTGGTACGTGTTGAT |
| miR-34b-3p | GCGCGAATCACTAACTCCACT | AGTGCAGGGTCCGAGGTATT |
| miR-433-3p | GCGATCATGATGGGCTCCT | AGTGCAGGGTCCGAGGTATT |
| miR-34c-5p | CGCGAGGCAGTGTAGTTAGCT | AGTGCAGGGTCCGAGGTATT |
| miR-34c | GCGCGAATCACTAACCACACA | AGTGCAGGGTCCGAGGTATT |
| miR-431 | GCGTGTCTTGCAGGCCGT | AGTGCAGGGTCCGAGGTATT |
| miR-214-5p | CGCGTGCCTGTCTACACTTG | AGTGCAGGGTCCGAGGTATT |
| miR-411-3p | CGCGTATGTAACACGGTCCA | AGTGCAGGGTCCGAGGTATT |
| miR-299a-5p | GCGTGGTTTACCGTCCCAC | AGTGCAGGGTCCGAGGTATT |
| miR-154-5p | CGCGTAGGTTATCCGTGTTG | AGTGCAGGGTCCGAGGTATT |
| miR-134-5p | CGCGTGTGACTGGTTGACCA | AGTGCAGGGTCCGAGGTATT |
| U6 | GCTTCGGCAGCACATATACTAAAAT | CGCTTCACGAATTTGCGTGTCAT |

## Conclusions

In conclusion, our study demonstrates that hypoxia preconditioning in mice at an altitude of 5 km for 7 consecutive days, resulting in a daily exposure of 1 h, leads to a significant increase in the content of miR-34b-3p within circulating exosomes. Furthermore, we have identified that miR-34b-3p specifically targets the *Clock* gene, resulting in the inhibition of its expression. This regulatory mechanism ultimately influences the expression of the clock gene and subsequently impacts the proliferation and migration of NIH 3T3 cells. This study has elucidated a novel mechanism of hypoxia preconditioning in the regulation of circadian rhythm, proposing that exosome miR-34b-3p functions as an unrecognized molecule involved in modulating circadian rhythm. These findings offer a new avenue for developing protective strategies and therapeutic targets for circadian rhythm disorders.

## Materials and methods

### Ethics statements

The animal experimental procedures were carried out in accordance with the guidelines for the care and use of laboratory animals at Fourth Military Medical University.

### Cell culture

NIH 3T3 cells procured from the Type Culture Collection of the Chinese Academy of Sciences (Shanghai, China) were maintained in DMEM (HyClone, Logan, UT, USA) supplemented with 10% FBS (ZETA Life Inc., Menlo Park, CA, USA), 100 U/ml penicillin (Solarbio, Beijing, China), and 100 mg/ml; streptomycin (Solarbio, Beijing, China). The cells were cultured at 37°C in a humidified chamber with 5% $CO_2$. The experimental protocol involved exchanging the medium with a solution containing 50% horse serum (Thermo Scientific, New Zealand) and synchronizing the cells with serum-rich medium [supplemented with 50% horse serum (Thermo Scientific, New Zealand)] for 2 h, followed by replacement with 0.4% DMEM for the subsequent culture. NIH 3T3 cells in the hypoxic group (HYP) were cultured in a tri-gas incubator (Billups-Rothenberg Inc., Del Mar, CA, USA) with a gas mixture of 5% $CO_2$/94% $N_2$/1% $O_2$ in normal medium for 4 h, while cells in the normal oxygen group (NOR) were maintained in a standard incubator with a gas mixture of 5% $CO_2$/95% air. Cells were collected at 6-h intervals throughout a 36-h duration, beginning at the time of adding 50% horse serum at time = 0, in order to capture one circadian cycle. Following cell collection, they were stored at –80°C for subsequent experiments. Transfection of miRNA mimics (100 nmol/l), miRNA inhibitors (200 nmol/l), siRNAs (100 nmol/l), and their respective negative controls (100–200 nmol/l) were carried out using Lipofectamine RNAi MAX (Thermo, Carlsbad, CA, USA) in accordance with the manufacturer's guidelines.

### Animals and hypobaric hypoxia preconditioning

Eight-week-old male C57BL/6 mice were procured from the Center of Animal Experiment of Fourth Military Medical University in Xi'an, China, and housed in the Laboratory of Experimental Animal Centre under pathogen-free conditions (18–22°C, 12-h light/dark cycle) with ad libitum access to food and water. The mice were randomly assigned to two groups ($n = 30$ per group) for differential treatment. The study included two groups: the control group exposed to normal oxygen levels and the preconditioning group subjected to hypobaric hypoxia preconditioning. The preconditioning group consisted of mice that were placed in a hypobaric hypoxia chamber (Dyc-3000; Guizhou Feng Lei Aviation Machinery Co., Ltd, Guangzhou, China) and received 1-h daily hypobaric hypoxia preconditioning for 7 days. The mice were exposed to hypoxia at a progressively increased simulated altitude of 5000 m, with a relative sea-level oxygen content of 10.5%.

### Exosome isolation and identification

Our description and research on exosomes adhere to the MISEV2023 guidelines. Blood samples were collected from mice belonging to various experimental groups immediately following the final intervention. After collection, the blood samples underwent centrifugation at 2000 g for 15 min at 4°C to isolate plasma, followed by centrifugation at 10 000 g for 30 min at 4°C to eliminate residual cells and platelets. Subsequently, the samples underwent two rounds of centrifugation at 100 000 g for 60 min at 4°C to isolate exosomes. The resulting supernatant was filtered through a 0.22 μm PVDF filter (Millipore, SLGP033RB) and subjected to two additional rounds of ultracentrifugation at 100 000 g for 90 min to collect the pellet, which was then resuspended in 80–160 μl of PBS. Plasma exosomes were isolated using the ExoQuick Plasma prep and the Exosome Precipitation Kit in accordance with the manufacturer's guidelines (System Biosciences). The filtered culture medium was combined with ExoQuick exosome precipitation solution at a ratio of 5:1 and incubated for more than 12 h, followed by centrifugation at 1500 g for 30 min. Additionally, serum exosomes were isolated using the exosomes isolation reagent (System Biosciences). The reagent was applied to serum samples and incubated overnight at 4°C before centrifugation of the serum samples (250 μl) at 2000 g for 30 min. The isolated exosomes were resuspended in 200 μl of PBS for subsequent experimentation. Nanoparticle tracking analysis (NTA) was conducted using the ZETA-VIEW particle tracker (Particle Metrix, Germany) to assess the exosomes by measuring the rate of Brownian motion for calculating nanoparticle concentrations and size distribution. Additionally, scanning electron microscopy (HITACHI, SU8100, Japan) was employed to examine the morphology of the exosomes. The protein concentration of the exosomes was determined using the bicinchoninic acid (BCA) protein assay kit (Beyotime, Shanghai, China). The Western blotting analysis was utilized to examine the expression of exosome-specific biomarkers TSG101 and CD81.

### RNA extraction and quantitative real-time PCR

Total RNA was extracted from distinct cohorts of NIH 3T3 cells subjected to various treatments, followed by homogenization in TRIzol reagent (Life Technologies, New York, NY, USA) and subsequent extraction and precipitation using chloroform and isopropanol. The resulting supernatants were removed post-centrifugation, and the RNA pellet was resuspended in RNase-free water and stored at –80°C for subsequent analysis. Subsequently, complementary DNA (cDNA) was synthesized utilizing random primers. PCR reactions were carried out in a 25 μl reaction volume, consisting of 12.5 μl SYBR Premix Ex Taq (Takara, Tokyo, Japan), 1 μl of each primer, 0.5 μl cDNA template, and conducted on a BioRad Real-Time PCR System using a thermal cycling program of 95°C for 5 s and 60°C for 34 s for a total of 40 cycles. Triplicate samples were normalized to GAPDH, the relative miRNAs samples were normalized to U6. Specific primers for *Clock*, *Bmal1*, *Per1*, GAPDH, miRNAs and U6 were synthesized by BioSune Company (Shanghai, China). The *Bmal1* cDNA was amplified using a set of primers (forward 5′-TTCCCTCGGTCACATCCTAC-3′ and reverse 5′-CCAACCCATACACAGAAGCA-3′). The primers sequences for quantitative real-time PCR were described in Table 1.

### Western blotting

The cells from various treatment groups underwent two washes with ice-cold PBS before being solubilized in RIPA buffer (Beyotime Biotechnology, Shanghai, China) supplemented with 1 mmol/l PMSF on ice. The protein concentration of each sample was determined using the BCA Protein Assay kit (Thermo Scientific, Fremont, CA, USA). Subsequently, NIH 3T3 cell lysates were separated by SDS-PAGE, with each lane loaded with 20 μg of protein and transferred onto a PVDF membrane. The membranes were subsequently blocked with 5% skim milk for a duration of 2 hours, followed by incubation with primary antibodies (CD81, TSG101, CLOCK, Akt, p-AKT, PI3K, p-PI3K, and GAPDH at a dilution of 1:2000 in 5% skim milk) overnight at 4°C. Subsequently, the membranes were exposed to peroxidase-conjugated secondary antibodies at room temperature for 1 h and washed thrice with PBS containing 0.1% Tween-20 (PBST). The chemiluminescent HRP substrate reagent (Millipore, MA, USA) was utilized for signal visualization, and Image J software was employed for image analysis.

### Wound healing assay

Straight lines were delineated across the underside of six-well culture plates using a marker pen. NIH 3T3 cells treated with varying conditions were then seeded at a density of $5 \times 10^5$ cells per well in the plates, and a pipette tip was employed to create scratches in the confluent cell monolayer. These scratches were made perpendicular to the previously drawn horizontal lines. Subsequently, the plates were washed with serum-free medium to eliminate any detached cells, and then cultured in DMEM (HyClone, Logan, UT, USA) supplemented with 10% FBS (ZETA Life Inc., Menlo Park, CA, USA) and varying concentrations of exosomes for a duration of 48 h. The images were obtained at time points 0 hour and 48 h using an inverted microscope (Olympus IX2-ILL100, Japan). The measurement of wound width was conducted using Image J software, and the experiment was replicated three times.

### Cell viability assay

The viability of NIH 3T3 cells was assessed using the Cell Counting Kit-8 (CCK-8) assay. A total of $8 \times 10^3$ cells suspended in 100 μl were plated in 96-well plates and allowed to attach at 37°C in a humidified chamber with 5% $CO_2$ prior to treatment. Following cell attachment, the medium was removed and replaced with 200 μl of medium containing exosomes at concentration of 25, 50, 100, and 200 μg/ml for different treatment groups. The cells were then incubated for 24, 48, and 72 h. Subsequently, 20 μl of CCK8 solution (Solarbio, China) was added to each well and incubated for an additional 2 h at 37°C. The optical density at 450 nm was measured using a microplate reader (Thermo, MULTISKAN MK3, USA). Each sample was analyzed in duplicate, and the experiment was replicated three times.

### miRNA library construction and sequencing

The miRNA library preparation and sequencing were outsourced to a commercial service provider (Ribobio, China). Briefly, total RNAs were isolated from exosomes purified from 2 ml of plasma. Adaptors were added to both the 3′ and 5′ ends of the RNA molecules, followed by reverse transcription and polymerase chain reaction amplification. The resulting PCR products, derived from RNA molecules ranging from 18 to 30 nucleotides, were purified via electrophoresis and sequenced using the Illumina HiSeq 2500 platform.

### Dual-luciferase reporter assay

NIH 3T3 cells were plated in 48-well plates at a density of $\sim 8 \times 10^4$ cells per well. When they reached 70–90% confluency on the second day, a transfection mixture containing miR-34b-3p mimics (or negative control), pGL3-Clock 3′ UTR (wild type or mutant), and pRL-TK at concentrations of 20 pmol, 100 ng, and 10 ng, respectively, was prepared. Transfection was conducted in a single well of a 48-well plate using Lipofectamine TM 2000 (0.8 μl/well). Each experimental group was replicated in three wells. The growth medium was replaced with fresh DMEM supplemented with 10% FBS 4–6 h after transfection. Following a 48-h incubation period, the cells from each well were lysed using the reagents provided in the kit. Subsequently, the entire lysate was transferred to a new EP tube and centrifuged at 12 000 rpm for 15 min at 4°C. After centrifugation, 5 μl of the supernatant was transferred to a new 1.5 ml EP tube in a light-protected environment, followed by the addition of 10 μl of LAR II substrate at ambient temperature. The contents of the EP tube were homogenized for analysis, and subsequently, 10 μl of Stop&Glo substrate at room temperature was introduced for re-analysis post-mixing. The ratio of the resultant values from the analytical procedure denoted the relative fluorescence intensity of the specimen.

### Statistics analysis

Plotting of statistics and statistical analyses were performed in GraphPad Prism 8.3.0. Comparisons between groups were undertaken using two-way ANOVA. Results were expressed as the mean ± standard deviation (SD) from at least three subjects per group. $P < .05$ was considered statistically significant.

## Author contributions

Xingcheng Zhao (Conceptualization, Project administration, and Funding acquisition, Writing—original draft, Writing—review and editing, Visualization and supervision), Jin Ma (Conceptualization, Project administration, and Funding acquisition, Writing—review and editing, Visualization and supervision), Yiquan Yan (Writing—original draft, Methodology, Software, Validation, Formal Analysis, and Investigation, Data curation, Writing—review and editing), Fengzhou Liu (Methodology, Software, Validation, Formal Analysis, and Investigation, Data curation), Tongmei Zhang (Methodology, Software, Validation, Formal Analysis, and Investigation, Data curation), Yateng Tie (Resources), Rui Wang (Resources), and Qi Yang (Resources). All authors have read and agreed to the published version of the manuscript.

Conflict of interest: None declared.

## Funding

This work was supported by grants from the National Natural Science Foundation of China (82304019, 81803098), Military Medicine and Aviation Medicine Major Science and Technology Project of Fourth Military Medical University (2022ZZXM013).

## Data availability

The original contributions presented in the study are included in the article. Further inquiries can be directed to the corresponding author/s.

## References


1. Huang W, Ramsey KM, Marcheva B *et al*. Circadian rhythms, sleep, and metabolism. *J Clin Invest* 2011;**121**:2133–41.
2. Merrow M, Brunner M. Circadian rhythms. *FEBS Lett* 2011;**585**:1383.
3. Zhou L, Zhang Z, Nice E *et al*. Circadian rhythms and cancers: the intrinsic links and therapeutic potentials. *J Hematol Oncol* 2022;**15**:21.
4. Man AWC, Li H, Xia N. Circadian rhythm: potential therapeutic target for atherosclerosis and thrombosis. *Int J Mol Sci* 2021;**22**:676.
5. Dragoi CM, Nicolae AC, Ungurianu A *et al*. Circadian rhythms, chrononutrition, physical training, and redox homeostasis-molecular mechanisms in human health. *Cells* 2024;**13**:138.
6. Patke A, Young MW, Axelrod S. Molecular mechanisms and physiological importance of circadian rhythms. *Nat Rev Mol Cell Biol* 2020;**21**:67–84.
7. Bartman CM, Eckle T. Circadian-hypoxia link and its potential for treatment of cardiovascular disease. *Curr Pharm Des* 2019;**25**:1075–90.
8. Hogenesch JB, Gu YZ, Jain S *et al*. The basic-helix-loop-helix-PAS orphan MOP3 forms transcriptionally active complexes with circadian and hypoxia factors. *Proc Natl Acad Sci U S A* 1998;**95**:5474–79.
9. Wu YL, Tang DB, Liu N *et al*. Reciprocal regulation between the circadian clock and hypoxia signaling at the genome level in mammals. *Cell Metab*. 2017;**25**:73–85.
10. Adamovich Y, Ladeuix B, Golik M *et al*. Rhythmic oxygen levels reset circadian clocks through HIF1α. *Cell Metab*. 2017;**25**:93–101.
11. Adamovich Y, Ladeuix B, Sobel J *et al*. Oxygen and carbon dioxide rhythms are circadian clock controlled and differentially directed by behavioral signals. *Cell Metab* 2019;**29**:1092–103e3.
12. Li X, Fang S, Wang S *et al*. Hypoxia preconditioning of adipose stem cell-derived exosomes loaded in gelatin methacryloyl (GelMA) promote type H angiogenesis and osteoporotic fracture repair. *J Nanobiotechnology* 2024;**22**:112.
13. Sohi GK, Farooqui N, Mohan A *et al*. The impact of hypoxia preconditioning on mesenchymal stem cells performance in hypertensive kidney disease. *Stem Cell Res Ther* 2024;**15**:162.
14. Yang Y, Wu Y, Yang D *et al*. Secretive derived from hypoxia preconditioned mesenchymal stem cells promote cartilage regeneration and mitigate joint inflammation via extracellular vesicles. *Bioact Mater* 2023;**27**:98–112.
15. Manella G, Aviram R, Bolshette N *et al*. Hypoxia induces a time- and tissue-specific response that elicits intertissue circadian clock misalignment. *Proc Natl Acad Sci U S A* 2020;**117**:779–86.
16. Krylova SV, Feng D. The machinery of exosomes: biogenesis, release, and uptake. *Int J Mol Sci* 2023;**24**:1337.
17. Liang Y, Duan L, Lu J *et al*. Engineering exosomes for targeted drug delivery. *Theranostics* 2021;**11**:3183–95.
18. Pegtel DM, Gould SJ. Exosomes. *Annu. Rev. Biochem* 2019;**88**:487–514.
19. Rahimian N, Nahand JS, Hamblin MR *et al*. Exosomal MicroRNA Profiling. *Methods Mol Biol* 2023;**2595**:13–47.
20. Yu X, Odenthal M, Fries JW. Exosomes as miRNA carriers: formation-function-future. *Int J Mol Sci* 2016;**17**:2028.
21. Hu N, Cai Z, Jiang X *et al*. Hypoxia-pretreated ADSC-derived exosome-embedded hydrogels promote angiogenesis and accelerate diabetic wound healing. *Acta Biomater* 2023;**157**:175–86.
22. Khalyfa A, Ericsson A, Qiao Z *et al*. Circulating exosomes and gut microbiome induced insulin resistance in mice exposed to intermittent hypoxia: Effects of physical activity. *EBioMedicine* 2021;**64**:103208.
23. Li L, Mu J, Zhang Y *et al*. Stimulation by exosomes from hypoxia preconditioned human umbilical vein endothelial cells facilitates mesenchymal stem cells angiogenic function for spinal cord repair. *ACS Nano* 2022;**16**:10811–23.
24. Ge L, Xun C, Li W *et al*. Extracellular vesicles derived from hypoxia-preconditioned olfactory mucosa mesenchymal stem cells enhance angiogenesis via miR-612. *J Nanobiotechnology* 2021;**19**:380.
25. Zhu LP, Tian T, Wang JY *et al*. Hypoxia-elicited mesenchymal stem cell-derived exosomes facilitates cardiac repair through miR-125b-mediated prevention of cell death in myocardial infarction. *Theranostics* 2018;**8**:6163–77.
26. Kuhestani-Dehaghi B, Amirpour M, Nabigol M *et al*. Evaluating the effect of acute myeloblastic leukemia-derived exosomes on the human bone marrow mesenchymal stromal cell proliferation. *Mol Biol Rep* 2024;**52**:62.
27. Song Y, You Y, Xu X *et al*. Adipose-derived mesenchymal stem cell-derived exosomes biopotentiated extracellular matrix hydrogels accelerate diabetic wound healing and skin regeneration. *Adv Sci* 2023;**10**:e2304023.
28. Wang R, Yan Y, Tie Y *et al*. Hypoxic acclimatization training improves the resistance to motion sickness. *Front Neurosci* 2023;**17**:1216998.
29. Hou Z, Qin X, Hu Y *et al*. Longterm Exercise-Derived Exosomal miR-342-5p: A Novel Exerkine for Cardioprotection. *Circ Res* 2019;**124**:1386–400.
30. Saliminejad K, Khorram Khorshid HR, Soleymani Fard S *et al*. An overview of microRNAs: biology, functions, therapeutics, and analysis methods. *J Cell Physiol* 2019;**234**:5451–65.


Environmental Epigenetics, 2025, 11(1), dvaf002 , DOI: https://doi.org/10.1093/eep/dvaf002, Advance Access Publication 17 March 2025, RESEARCH ARTICLE

Received 7 August 2024; Revised 7 January 2025; Accepted 17 February 2025